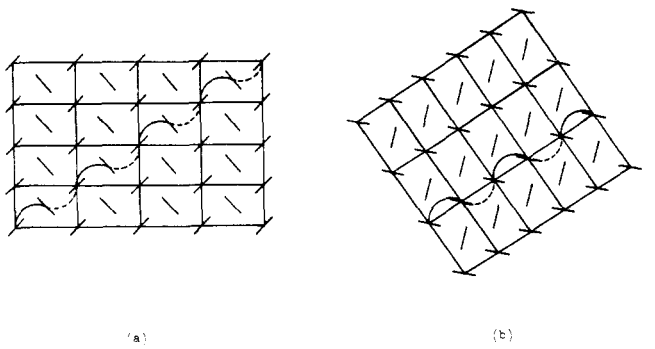

**Figure 4.** Possible conversion from (a) (110) to (b) (200) folding in which fold plane orientation in space is unchanged.

$CH_2$ rocking modes which is observed in pure PEH (Figure 2) as well as the mixed crystals (Table I) in the vicinity of 100°C. This decrease must be due to, on the average, weaker inter-chain interactions, which could arise from small increases in the unit cell dimensions. The latter could result from the freezing in of "defective" chain orientations that are not completely eliminated until higher annealing temperatures are reached. It is interesting to note that evidence for such frozen-in disorder has been obtained from X-ray diffraction studies.[19]

The existence of the above dip in $CH_2$ rocking mode splitting with annealing temperature makes it unlikely that the mechanism of annealing can be explained in terms of a partial melting and recrystallization, as has been suggested.[18,20] If the latter were true, then, since the splitting for melt-crystallized polymer is higher than that for single crystals,[15] we would expect a continuous increase in the splitting as we pass through the transition region and form more (melt) recrystallized polymer. This is not observed, and therefore we must suppose that the reorganization of chains does not proceed through a melt state.

The above results suggest an important conclusion which emerges from these studies, namely that (110) folding in solution-grown single crystals comprises a frozen-in metastable state compared to that which is most stable in the bulk polymer. In other words, crystallization in the presence of this solvent has led to a form of fold organization which, although favored under these circumstances, is not maintained when the chains are given the freedom to move and to adjust to a minimum free-energy state in the bulk. This transformation from (110) to (200) folding upon annealing provides further support for the existence of folding with adjacent re-entry in crystalline poly(ethylene).

**Acknowledgment.** This research was supported by National Science Foundation Grant MPS75-05239.

### References and Notes

(1) A. Keller, *Philos. Mag.*, **2**, 1171 (1957).
(2) P. J. Flory, *J. Am. Chem. Soc.*, **84**, 2857 (1962).
(3) L. Mandelkern, *J. Polym. Sci., Part C*, **15**, 129 (1966).
(4) A. Keller, *Kolloid-Z.*, **197**, 98 (1964).
(5) A. Keller, *Rep. Prog. Phys., Part 2*, **31**, 623 (1968).
(6) A. Keller, *MTP Int. Rev. Sci.: Phys. Chem., Ser. 1*, **8**, 105 (1973).
(7) P. H. Lindenmeyer, *J. Polym. Sci., Part C*, **1**, 5 (1963).
(8) T. Kawai, T. Goto, and H. Maeda, *Kolloid-Z.*, **223**, 117 (1968).
(9) M. Tasumi and S. Krimm, *J. Polym. Sci., Part A-2*, **6**, 995 (1968).
(10) M. I. Bank and S. Krimm, *J. Polym. Sci., Part A-2*, **7**, 1785 (1969).
(11) F. C. Stehling, E. Ergos, and L. Mandelkern, *Macromolecules*, **4**, 672 (1971).
(12) S. Krimm and J. H. C. Ching, *Macromolecules*, **5**, 209 (1972).
(13) J. H. C. Ching and S. Krimm, *J. Appl. Phys.*, in press.
(14) S. Krimm, J. H. C. Ching, and V. L. Folt, *Macrolecules*, **7**, 537 (1974).
(15) S. Krimm, "Proceedings of the International Symposium on Macromolecules", Rio de Janeiro, Elsevier Publishing Co., New York, N.Y., 1974, p 107.
(16) M. I. Bank and S. Krimm, *J. Polym. Sci., Part B*, **8**, 143 (1970).
(17) A. Peterlin, *Polym. J.*, **6**, 25 (1965).
(18) E. W. Fischer and F. G. Schmidt, *Angew. Chem.*, **74**, 551 (1962).
(19) K. Iohara, K. Imada, and M. Takayanagi, *Polym. J.*, **4**, 239 (1973).
(20) H. A. Stuart, *Pure Appl. Chem.*, **5**, 743 (1962).

# Contribution of Vibrational Free Energy Term to Stability of Polymethylene Crystal Lattices

**Masamichi Kobayashi* and Hiroyuki Tadokoro**

*Department of Polymer Science, Faculty of Science, Osaka University, Toyonaka, Osaka, 560 Japan.* *Received July 2, 1975*

ABSTRACT: The vibrational terms of the thermodynamical functions, the internal energy, the entropy, and the Helmholtz's free energy of the orthorhombic, monoclinic, and triclinic modifications of polymethylene have been calculated in a harmonic approximation by means of normal modes treatment of the crystal lattices using Lennard-Jones type and Buckingham type intermolecular hydrogen–hydrogen potential functions. The calculated results for the orthorhombic form reproduce well the thermodynamical functions derived from thermal measurements. The vibrational free energy term of the orthorhombic form is found to be 0.5–0.3 kJ/mol per $CH_2$ unit less than that of the monoclinic and triclinic forms at 300°K. The value seems large enough to compensate for the static potential energy term which has been estimated as 0.15 kJ/mol per $CH_2$ unit higher in the orthorhombic form than in the monoclinic form. Thus, the vibrational free energy term contributes to the thermodynamical stability of the orthorhombic lattice of polymethylene under the normal conditions. The free energy of the liquid phase has been derived from the thermal data reported and the results of the present calculation.

As is well-known polyethylene crystallizes into an orthorhombic form under ordinary conditions.[1] Another crystal modification of a monoclinic system has been found to appear when the sample specimen is put under stress.[2,3] Thus, the monoclinic form may be metastable under normal conditions. Yemni and McCullough[4] tried to clarify the transition mechanism between these two crystal forms by calculating the static potential energy of the polymethylene crystal with variations in the cell constants and the orientations of the chains. In contrast to the experimental findings, the monoclinic form was found to be more stable by about 0.15 kJ/mol per $CH_2$ unit than the orthorhombic

Table I
Crystallographic Data of Three Crystal Modifications of Polymethylene Adopted for the Present Calculation.

| Crystal system | Orthorhombic[a] | Monoclinic[b] | Triclinic[c] |
|---|---|---|---|
| Lattice constants | $a$ = 7.47 Å<br>$b$ = 4.97 Å<br>$c$(f.a.)[d] = 2.515 Å | $a$ = 4.79 Å<br>$b$ = 8.09 Å<br>$c$(f.a.) = 2.515 Å<br>$\gamma$ = 107.9° | $a$ = 4.285 Å<br>$b$ = 4.82 Å<br>$c$(f.a.) = 2.515 Å<br>$\alpha$ = 79.8°<br>$\beta$ = 71.9°<br>$\gamma$ = 107.3° |
| Space group | $Pnam$-$D_{2h}^{16}$ | $A2/m$-$C_{2h}^{3}$ | $P1$-$C_i^1$ |

[a] Based on the Smith's cell.[9] [b] After Seto et al.[3] [c] Derived from the data of $n$-octadecane after Nyburg and Lüth.[11] [d] f.a.: fiber axis.

form. Although the value itself varies, more or less, depending on the values of parameters assumed in the calculation, a similar tendency has been recognized by the authors from a static potential energy calculation in a different way.[5] Therefore, it may be supposed that the actual stability of the two crystal forms of polyethylene cannot be reproduced by taking into account the static potential energy alone.

A great number of papers has been published in which a good deal of effort has been made to reproduce actual crystal structures by minimizing static potential energy. However, the free energy term due to the vibrational freedom of the molecules in the crystal lattice plays an essentially important role in the stability of the crystalline phase. Because of the necessity of a long computation time the contribution of the vibrational free energy term has been ignored in most cases and taken into account only in very limited cases of simple lattices containing only one atom in the unit cell, such as the face-centered cubic lattices of the inert gas solids,[6,7] or it has been included in the energy calculation in an approximate way.[8]

In the present work, for three crystal forms of polymethylene, i.e., orthorhombic (referred to as o-PE), monoclinic (m-PE), and triclinic (t-PE), the frequency distribution functions are obtained by calculating dispersion relations of the normal frequencies in the first Brillouin zone of the three-dimensional reciprocal space in the harmonic approximation, and the thermodynamical functions, such as the Helmholtz's free energy $F$, the internal energy $E$, the entropy $S$, and the heat capacity $C_v$, are derived. The thermal stabilities of these crystal forms are discussed in relation to the calculated thermodynamical functions.

## Method of Calculation

The cell constants and the space groups of the three crystal forms adopted for the present work are summarized in Table I and Figure 1. As for the orthorhombic cell the lattice parameters given by Smith[9] were chosen as used in the previous work by Tasumi and Shimanouchi.[10] The lattice parameters of m-PE refer to those of Seto et al.[3] The triclinic subcell was derived from the crystallographic data of $n$-octadecane after Nyburg and Lüth[11] (see Appendix). The molecular parameters, i.e., the bond lengths and the valence angles, given in the literature are different in the three crystal forms. However, in order to eliminate the effects due to different molecular structure an identical planar zigzag molecular model was adopted for the three crystal forms in which the C–C bond length of 1.54 Å, the C–H bond length of 1.09 Å, and the tetrahedral angle for all the valence angles were assumed. Therefore, the assumed cell dimensions ($c$ dimension) are somewhat modified from the published values.

The values of the intramolecular force constants of a valence force field type were transferred directly from

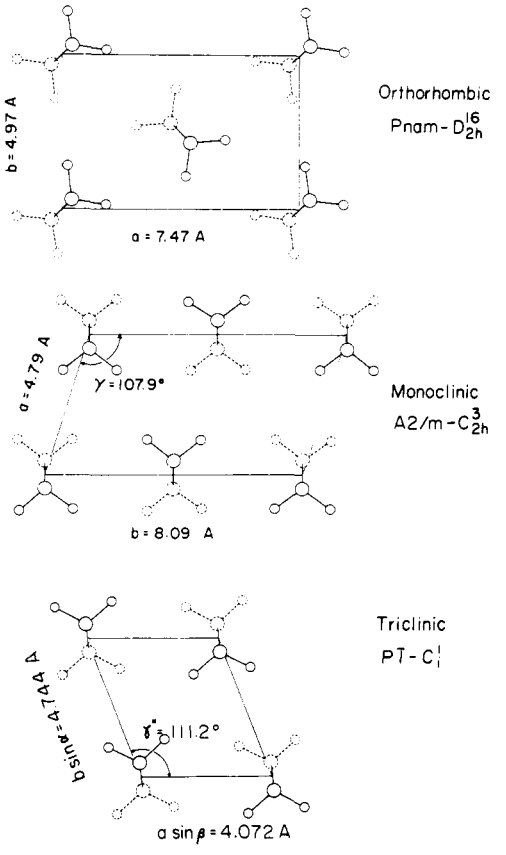


**Figure 1.** Crystal structures of three crystal forms of polymethylene.

Schachtschneider and Snyder[12] (the set II in the Table IV of ref 12). They reproduce the infrared and Raman frequencies of o-PE within a maximum deviation of 3.0%. As for the intermolecular forces, interactions were taken into account between two hydrogen atoms separated from each other by a distance less than 3.0 Å. Two types of intermolecular force constant are used as shown in Figure 2: one (solid line) is given as the second derivative of the repulsive term of the Lennard-Jones type H···H potential function[13] with respect to the interatomic distance (potential function I),

$$F(\text{H}\cdots\text{H})\ (\text{mdyn/A}) = 4836r^{-14}$$

($r$: H···H distance in ångström units)

and the other (broken line) has been proposed by Harada and Shimanouchi[14] for reproducing the vibrational frequencies of crystalline benzene (potential function II)

$$F(\text{H}\cdots\text{H})(\text{mdyn/A}) = 163\exp(-3.534r)$$

For each crystal form, the normal frequencies were computed for the wavenumber vector $\mathbf{k} = (k_a,k_b,k_c)$, or the phase angle $\delta = (\delta_a,\delta_b,\delta_c) = 2\pi\mathbf{k}$, within the first Brillouin zone of the reciprocal space at the interval of 1.5° for $\delta_c$ and 90° for $\delta_a$ and $\delta_b$. The method of normal mode calculation has been described in previous papers.[15,16] The computation time has been saved by solving the secular equations by means of the perturbation technique.[17] The frequency distribution functions in the frequency range lower than 600 $cm^{-1}$ were obtained by the sampling method at the interval of 5 $cm^{-1}$.

The thermodynamical functions $E$, $S$, $F$, and $C_v$ are calculated according to the equations[18]

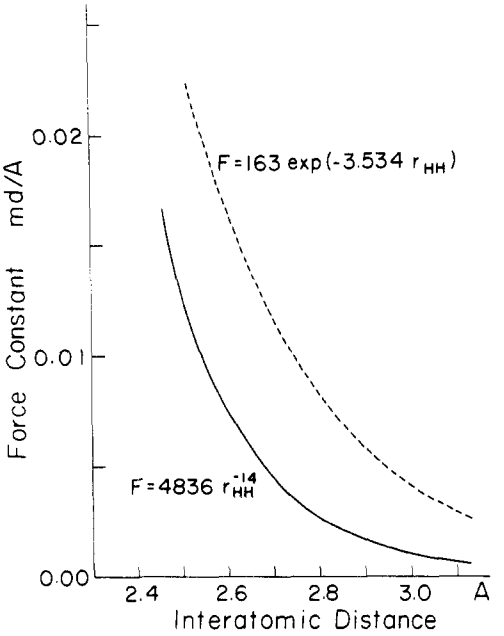


**Figure 2.** Hydrogen–hydrogen intermolecular potential functions derived from the repulsive term of a Lennard-Jones type H···H potential[13] (solid curve referred to as potential function I), and from the repulsive term of a Buckingham type H···H potential[14] (broken curve, potential function II).

$$E = (1/N) \sum_{\mathbf{k},j} \hbar\omega_j(\mathbf{k})\{[\exp(\hbar\omega_j(\mathbf{k})/kT) - 1]^{-1} + (1/2)\}$$

$$S = (k/N) \sum_{\mathbf{k},j} \left\{ \frac{\hbar\omega_j(\mathbf{k})}{2kT} \coth [\hbar\omega_j(\mathbf{k})/2kT] - \ln [2 \sinh (\hbar\omega_j(\mathbf{k})/2kT)] \right\}$$

$$F = (kT/N) \sum_{\mathbf{k},j} \ln \{2 \sinh [\hbar\omega_j(\mathbf{k})/2kT]\}$$

$$C_v = (k/N) \sum_{\mathbf{k},j} [\hbar\omega_j(\mathbf{k})/2kT]^2/\sinh^2 [\hbar\omega_j(\mathbf{k})/2kT]$$

where $N$ denotes the number of unit cells (or the number of points in the reciprocal space whose frequencies are computed), $\omega_j(\mathbf{k})$ the circular normal frequency of the $j$th branch with the wavenumber vector $\mathbf{k}$, $\hbar$ the Planck's constant divided by $2\pi$, $k$ the Boltzmann's constant, and $T$ the absolute temperature.

In the calculation of $E$, $S$, and $F$ the contribution of the molecular modes in the high-frequency region was taken into account. The calculated heat capacities do not include the contribution of the high-frequency molecular modes, since they were obtained from the frequency distribution functions lower than 600 $cm^{-1}$.

## Results and Discussion

Some examples of the calculated dispersion relations for the three crystal forms are shown in Figure 3, where the dispersions along the symmetry axis of $(0,0,\delta_c)$ are given for the lowest eight (for o-PE) or four (for m-PE and t-PE) branches in the frequency range lower than 300 $cm^{-1}$. Here, the frequency branches are separated, for convenience, into the right and left sides of the point of $(0,0,\pi)$. The results shown here are obtained by using the H···H potential function I. Use of the potential function II shifts the branches slightly to the higher frequency side. In the low-frequency region the three crystal forms each give characteristic dispersions, reflecting the respective molecular packing and space group symmetry.

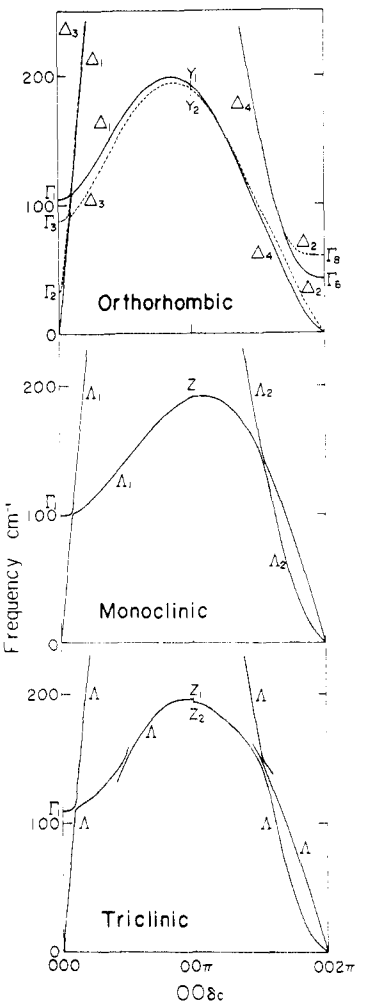


**Figure 3.** Dispersion relations of low-frequency branches of three crystal forms of polymethylene, calculated by using the H···H potential function I.

The symmetry of the so-called Γ point in reciprocal space, the point (0,0,0) or $(0,0,2\pi)$ in Figure 3, is identical with that of the point group isomorphous to the space group of the lattice: $D_{2h}$ for o-PE, $C_{2h}$ for m-PE, and $C_i$ for t-PE. Except for the Γ point and the point of $(0,0,\pi)$, the $(0,0,\delta_c)$ axis has the symmetry (**k**-group symmetry) of $C_{2v}$ for o-PE,[17] $C_2$ for m-PE, and $C_1$ for t-PE. The figures beside the curves denote the symmetry species of the **k** group of the branches. The notations are in accordance with Bouchaert, Smoluchowski, and Wigner.[19,20] It should be noted that the branches intersect each other only if they belong to different symmetry species of the **k** group. The **k** group at the point of $(0,0,\pi)$ for o-PE and m-PE has the symmetry of $D_{2h}$ and $C_{2h}$, respectively, but consists of doubly degenerate species in contrast to the corresponding point group. Therefore, two branches which are in opposite sides of the figure coincide with each other at the point $(0,0,\pi)$. In the case of t-PE, the **k**-group symmetry of this point is $C_i$ and the two symmetry species are both one dimensional. All the branches give, therefore, different frequencies at the points.

For checking adequacy of the intermolecular potential functions used here the calculated optically active lattice mode frequencies are compared with the observed ones in Table II. The assignment of the $B_{1u}$ mode to the infrared band at 73 $cm^{-1}$ (at room temperature) has been well-established. Another infrared active lattice mode of $B_{2u}$ has been observed as a very weak absorption at 109 $cm^{-1}$ (at 2 K) by Dean and Martin.[26] As for the Raman active libra-

Table II
Optically Active Lattice Mode Frequencies of Orthorhombic Polyethylene

| Species | Obsd, $cm^{-1}$ | | Calcd, $cm^{-1}$ (room temp) | |
|---|---|---|---|---|
| | Room temp | Low temp | Potential I | Potential II |
| $A_g$ | 105[a] | 133 (at 77 K)[a] | 104 | 181 |
| $B_{3g}$ | ca. 90[b] | 108 (at 77 K)[a] | 88 | 150 |
| $A_u$ | | | 31 | 59 |
| $B_{1u}$ | 72.5[c] | 79 (at 100 K)[c] | 42 | 77 |
| $B_{2u}$ | | 109 (at 2 K)[d] | 60 | 101 |

[a] R. T. Harley et al.[27] [b] M. Kobayashi et al.[28] [c] J. E. Bertie and E. Whalley[31] [d] G. Dean and D. H. Martin[26]

tional modes Harley et al.[27] assigned the Raman bands at 133 and 108 $cm^{-1}$ (both at 77 K) to the $A_g$ and $B_{3g}$, respectively, on the basis of the polarization measurement on single-crystal textured polyethylene samples. The same conclusion was obtained by the authors[28] from the polarized Raman spectra measured on a single crystal of $n$-$C_{36}H_{74}$. Although potential II reproduces well the $B_{1u}$ and $B_{2u}$ frequencies, better agreement for the $A_g$ and $B_{3g}$ frequencies is obtained by potential I. Potentials I and II give the calculated lattice mode frequency of the triclinic polyethylene lattice of 109 and 164 $cm^{-1}$, respectively. The observed value of the frequency has not yet been settled. Brunel and Dows[29] suggested that it was about 50 $cm^{-1}$ at 20 K from the Raman measurement of $n$-hexane, $n$-heptane, and $n$-octane. On the other hand Tasumi et al.[30] indicated that a plot of the observed frequencies measured on a number of triclinic $n$-paraffins against the phase angle gave a lattice mode frequency of about 100 $cm^{-1}$. Thus, both potentials I and II are not sufficient to interpret all the observed lattice mode frequencies, and it may be suggested that the most suitable intermolecular H···H potential function lies between them.

The frequency distribution functions in the frequency range lower than 600 $cm^{-1}$ for the three crystal forms are shown in Figure 4. The left and right halves of the figure represent the results obtained using the H···H potential functions I and II, respectively. The difference among the crystal forms is remarkable in the region lower than 200 $cm^{-1}$. Here we should note the error that arises from application of the perturbation technique. For the $(0,0,\delta_c)$ modes it was confirmed that the difference in frequency between those calculated with and without the perturbation technique was found to be less than 3 $cm^{-1}$ (for most modes it was about 1 $cm^{-1}$ or less) in the frequency range below 600 $cm^{-1}$. Therefore the effect of using the perturbation technique on the resulting frequency distribution functions may be ignored for the present purpose.

It is especially important to show how the calculated frequency distribution functions reproduce the observed thermodynamical quantities of the crystal. Unfortunately, however, the thermal data available for comparison with the present calculations are limited to those of o-PE. As for calculation of the heat capacity of o-PE, extensive studies have been made by Miyazawa and Kitagawa (see ref 17 and the pertinent literature cited therein). Very reliable experimental thermal data for o-PE were reported recently by Chang.[21] In Figure 5 the calculated heat capacity $C_v$ of o-PE is compared with his data for $C_p$ which are the values extrapolated to 100% crystallinity. The correction term due to thermal expansion, the $p\Delta V$ term, was estimated as negligible according to the empirical equation of thermal expansion for o-PE after Davis, Eby, and Colson.[22] The solid and broken curves correspond to the H···H potential I and

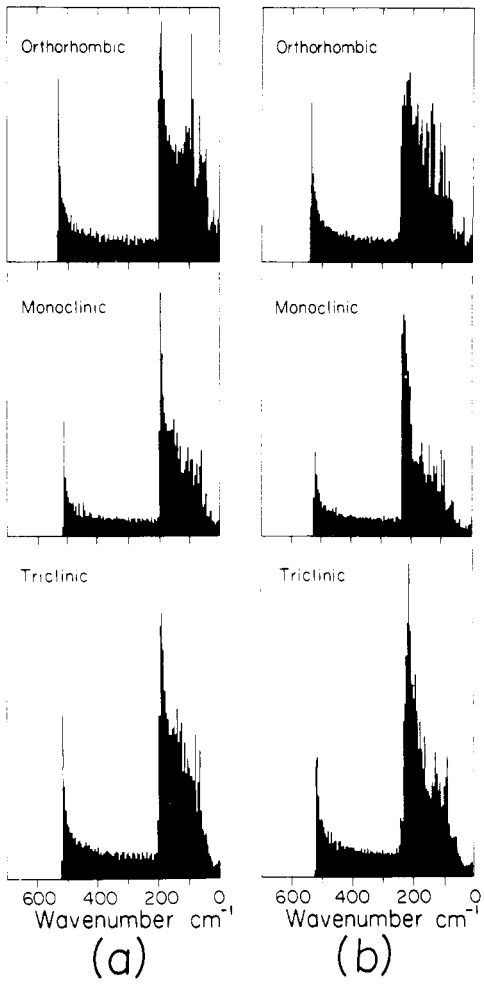


**Figure 4.** Frequency distribution functions of three crystal forms of polymethylene, (a) and (b) calculated by using the H···H potential functions I and II, respectively.

II, respectively, used for the calculation. The difference between the observed and calculated values above 100 K is due to the contribution of the molecular modes appearing in the frequency range higher than 700 $cm^{-1}$ which is neglected in the calculation of $C_v$. The observed values lie between two calculated curves. In Figure 6 the values of $S$, $E$, and $F$ derived from the observed thermal data are compared with the calculated results. The solid and broken curves have the same meaning as in Figure 5. The value of $E$ (or $F$) at the absolute zero temperature means the zero-point energy of the crystal. Since the absolute value of the zero-point energy cannot be evaluated from the thermal data, the observed points of $E$ and $F$ can be shifted along the ordinate. In Figure 6 the zero-point energy of the observed data is put conventionally on the calculated value of the solid curve. It can be shifted to that of the broken curve. The agreement between the observed and calculated values of the thermodynamical functions seems enough to conclude that the intermolecular H···H potential functions assumed in the present calculation are suitable to reproduce the thermodynamical properties of the o-PE crystal.

Then, the thermodynamical functions, $S$, $E$, and $F$, were calculated and compared with each other among the three crystal forms of polymethylene as shown in Figure 7. Here are shown the results calculated using the potential function I. A remarkable point in the figure is that the entropy term of o-PE is significantly higher than that of the other two crystal forms, while the heat term is nearly the same for the three forms. The difference in the zero-point energy

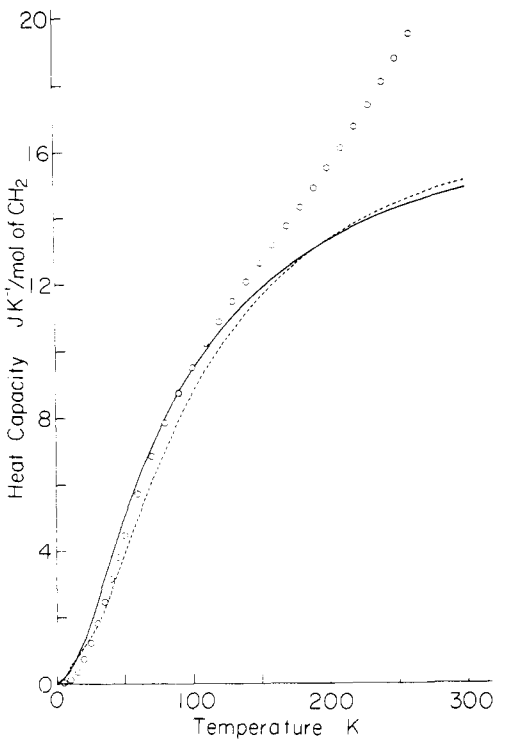


**Figure 5.** Heat capacity of orthorhombic polymethylene, calculated by using potential function I (—) and II (- - -), and the observed data (O) extrapolated to 100% crystallinity after Chang.[21]

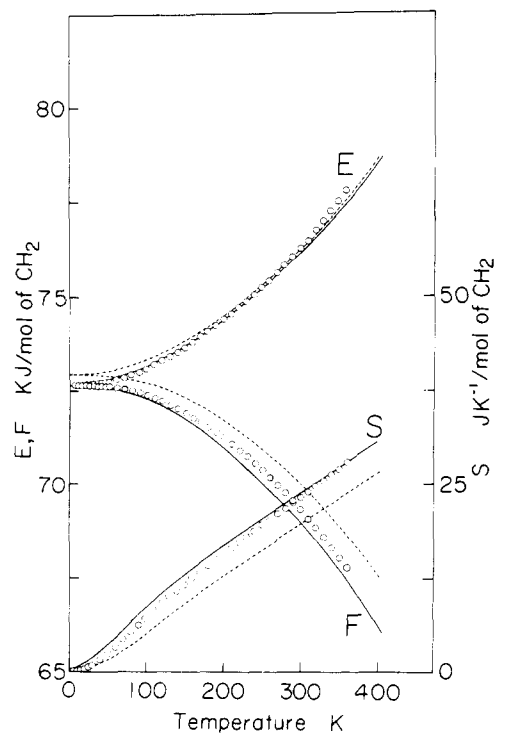


**Figure 6.** Thermodynamical functions, internal energy $E$, entropy $S$, and Helmholtz's free energy $F$ of orthorhombic polymethylene, calculated by using the H···H potential functions I (—) and II (- - -), and the observed data (O) extrapolated to 100% crystallinity after Chang.[21] The zero-point energy of the observed data can be chosen arbitrarily.

is less than 0.1 kJ/mol per $CH_2$ unit. As a result, at 300 K o-PE has the vibrational free energy of about 0.5 kJ/mol per $CH_2$ unit less than that of m-PE, the value being large enough to compensate the higher static potential energy (estimated as about 0.15 kJ/mol per $CH_2$ unit) of the former. The use of the potential function II gives the same trend with the rather smaller value of the free energy difference between o-PE and m-PE (about 0.3 kJ/mol per $CH_2$ unit at 300 K). Thus, it may be concluded that the vibrational free energy term contributes to the thermodynamical stability of the o-PE lattice under normal conditions. The triclinic form gives essentially the same results as the monoclinic form. This is reasonable from the fact that the chain packing in the two forms is quite similar to each other as shown in Figure 1.

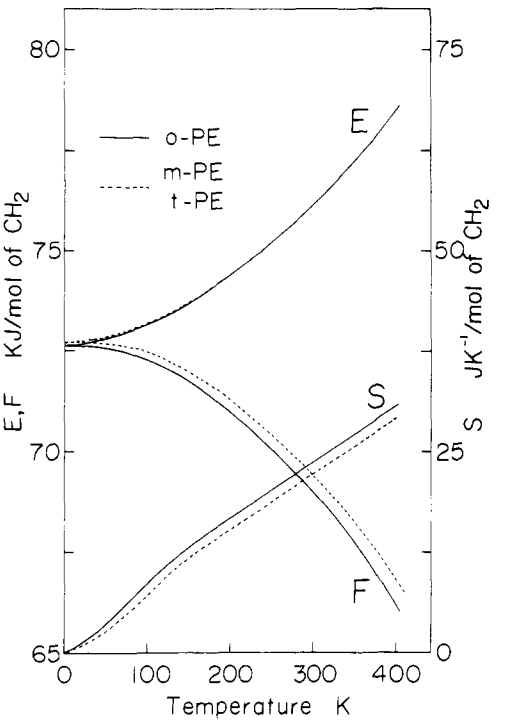


**Figure 7.** Thermodynamical functions, internal energy $E$, entropy $S$, and Helmholtz's free energy $F$ of orthorhombic (—) and monoclinic or triclinic (- - -) polymethylene, calculated by using the H···H potential function I.

By measuring the heat of fusion, Atkinson and Richardson[23] investigated the relative stability of the orthorhombic and triclinic systems of $n$-alkanes. The bulk free energy of fusion of the two systems showed that the orthorhombic form is about 0.05 kJ/mol per $CH_2$ unit more stable than the triclinic form in the temperature range from −35°C to the melting point. This observed value is somewhat smaller than that of the present calculation. If we assume that the static potential energy difference between o-PE and m-PE (or t-PE) does not change so much from the value of 0.15 kJ/mol per $CH_2$ unit through the whole temperature range, the total free energy curves of o-PE and m-PE intersect each other at a temperature around 100–150 K (see Figure 9); below this temperature the monoclinic (or triclinic) system becomes the stable form. This tendency is inconsistent with the result of Atkinson and Richardson where two curves slowly diverge as the temperature decreases.[23]

Actually the monoclinic phase of PE (which is referred to as a triclinic form by some workers[24]) has been found to appear when the sample specimen is treated at a low temperature. Teare and Holmes[24] ascribe the occurrence of the phase at low temperatures (or at high pressures) not to the thermodynamical stability of the phase but to "mistakes" (trapping of chains in an incorrect orientation) during rapid crystallization.

Taking into account the errors involved in the present calculation due to uncertainty in the atomic positions[16] and the potential function, and the correction terms due to the

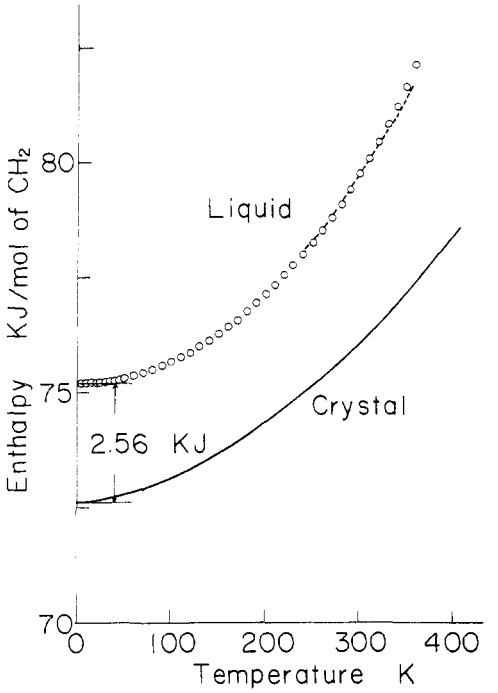


**Figure 8.** Enthalpy of liquid and orthorhombic polymethylene. Solid curve is for the orthorhombic lattice calculated by using the H···H potential function I, broken curve is for the liquid state derived from the solid curve and the observed data of heat of fusion after Atkinson and Richardson.[25] (○) Observed data of enthalpy ($H^a - H_0^a$) extrapolated to the 100% amorphous state after Chang.[21]

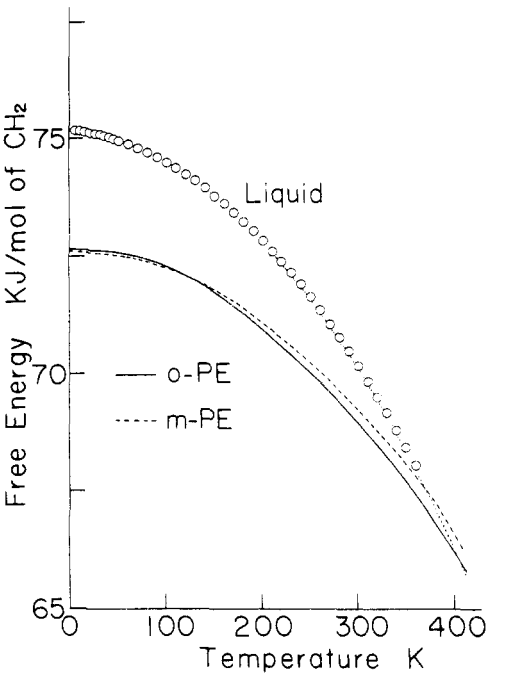


**Figure 9.** Free energy of liquid and crystalline polymethylene. Solid and Broken curves are for the orthorhombic and monoclinic (or triclinic) forms, respectively, calculated by using the H···H potential function I. Dotted curve is for the the liquid state obtained from the solid curve and the observed data of free energy of fusion after Atkinson and Richardson.[25] (○) The values obtained from the observed data of enthalpy ($H^a - H_0^a$) and entropy ($S^a - S_0^a$) of amorphous polymethylene after Chang[21] by using the values of the zero-point enthalpy $H_0^a$ = 2.56 kJ/mol per $CH_2$ unit and the residual entropy $S_0^a$ = 3.45 $JK^{-1}$/mol per $CH_2$ unit.

thermal expansion and the anharmonic character of vibrations, it is very difficult at this stage to decide whether the monoclinic phase appearing at low temperature is a thermodynamically stable phase or kinetically occurring metastable phase.

The free energy of the liquid (or amorphous) state of polyethylene was estimated by a rather conventional way. The values of ($S^a - S_0^a$) and ($H^a - H_0^a$) extrapolated to the 100% amorphous state after Chang[21] were used, the superscript a denoting "amorphous phase", $H_0^a$ the zero-point enthalpy, and $S_0^a$ the residual entropy at 0 K. Estimation of $H_0^a$ and $S_0^a$ was made by using the data of heat of fusion of crystalline polyethylene after Atkinson and Richardson[25] measured over the temperature range from −35°C to the melting point. The values of heat of fusion extrapolated to 100% crystallinity were added to the calculated enthalpy ($\simeq E$ neglecting the $p\Delta V$ term) of o-PE crystal, giving the enthalpy for the liquid phase $H^a$. The plotted curve of $H^a - H_0^a$ was adjusted by sliding it along the ordinate so as to get a good fitting with the enthalpy curve of the liquid state obtained above (Figure 8). By this means the zero-point enthalpy difference between the o-PE crystal and the liquid phase was evaluated as 2.56 kJ/mol per $CH_2$ unit.

The Gibbs' free energy of fusion for 100% crystallinity $\Delta G_\infty$ evaluated through eq 8 of ref 25 was added to the calculated free energy values of o-PE crystal, giving the free energy of the liquid phase $G^a$. The value of $S_0^a$ was so adjusted that the plots of $G^a = H^a - TS^a$ evaluated from the Chang's data of ($H^a - H_0^a$) and ($S^a - S_0^a$) fit the resulting curve of $G^a$ obtained above. The best fit was obtained for the value of $S_0^a$ = 3.45 $JK^{-1}$/mol per $CH_2$ unit as shown in Figure 9.

Using the free energy curve of the liquid phase we can estimate the melting points of the polyethylene crystals. Although the extrapolation to the melting region is rather difficult, the o-PE and m-PE lattices give the melting points of 141.2°C (this is the value given by eq 8 of ref 25) and about 100°C, respectively. The melting point of m-PE seems rather low compared to the reported extrapolated value of triclinic $n$-alkanes (138.0°C).[23] The discrepancy may be due to the terms ignored in the present calculation.

## Appendix

**Derivation of Subcell.** In the following derivation the original cell constants are represented as $a$, $b$, $c$, $\alpha$, $\beta$, and $\gamma$, and those of the subcell as $a_s$, $\alpha_s$, and so on. The original fractional coordinate $\mathbf{x}_j = (x_j,y_j,z_j)^T$ (the superscript T denotes transposition to a column vector) is transformed to a Cartesian coordinate $\mathbf{X}_j = (X_j,Y_j,Z_j)^T$ by the transformation matrix $\mathbf{U}$

$$\mathbf{U} = \begin{bmatrix} a & b\cos\gamma & c\cos\beta \\ 0 & b\sin\gamma & -c(\cos\beta\cos\gamma - \cos\alpha)/\sin\gamma \\ 0 & 0 & cK/\sin\gamma \end{bmatrix}$$

$$K = (1 - \cos^2\alpha - \cos^2\beta - \cos^2\gamma + 2\cos\alpha\cos\beta\cos\gamma)^{1/2}$$

where the $X$ axis is taken as parallel to the $a$ axis, the $Y$ axis is in the $ab$ plane, and the $Z$ axis is chosen so as to form a right-handed system.

The vector of the fiber axis of the subcell (the $c_s$ axis), i.e., the vector connecting two equivalent atoms separated from each other by the fiber identity period of the subcell (i.e., the vector C(9)–C(7) in the case of $n$-octadecane), is represented in terms of the Cartesian coordinate components as $\mathbf{R} = (R_X,R_Y,R_Z)^T$. A new Cartesian coordinate system $\mathbf{X}_j^s = (X_j^s,Y_j^s,Z_j^s)$ is constructed in which the fiber axis coincides with the $Z^s$ axis. The transformation matrix is given as

$$\mathbf{T} = \begin{bmatrix} \cos\theta\cos\phi & \cos\theta\sin\phi & -\sin\theta \\ -\sin\phi & \cos\phi & 0 \\ \sin\theta\cos\phi & \sin\theta\sin\phi & \cos\theta \end{bmatrix}$$

where

$$\cos\theta = R_Z/R$$

$$\cos\phi = R_X/R\sin\theta$$

$$R = (R_X^2 + R_Y^2 + R_Z^2)^{1/2}$$

The original fractional coordinate, say of the $j$th atom, is transformed to the new Cartesian coordinate as

$$\mathbf{X}_j^{\,s} = \mathbf{TU}\mathbf{x}_j$$

For an arbitrarily chosen reference atom the above transformation is applied to $\mathbf{x}_0 = (x_0,y_0,z_0)^T$, $\mathbf{x}_a = (x_0 + 1, y_0, z_0)^T$, and $\mathbf{x}_b = (x_0,y_0 + 1,z_0)^T$, giving $\mathbf{X}_0^{\,s}$, $\mathbf{X}_a^{\,s}$, and $\mathbf{X}_b^{\,s}$ from which the subcell dimensions are deduced as

$$a_s = a,\ b_s = b,\ c_s = R$$

$$\cos\alpha_s = (Z_b^{\,s} - Z_0^{\,s})/b_s$$

$$\cos\beta_s = (Z_a^{\,s} - Z_0^{\,s})/a_s$$

$$\cos\gamma_s = \{(X_a^{\,s} - X_0^{\,s})(X_b^{\,s} - X_0^{\,s}) + (Y_a^{\,s} - Y_0^{\,s})(Y_b^{\,s} - Y_0^{\,s}) + (Z_a^{\,s} - Z_0^{\,s})(Z_b^{\,s} - Z_0^{\,s})\}/a_s b_s$$

## References and Notes


(1) C. W. Bunn, *Trans. Faraday Soc.*, **35**, 482 (1939).
(2) H. Kiho, A. Peterlin, and P. H. Geil, *J. Appl. Phys.*, **35**, 1599 (1964).
(3) T. Seto, T. Hara, and K. Tanaka, *Jpn. J. Appl. Phys.*, **7**, 31 (1968).
(4) T. Yemni and L. McCullough, *J. Polym. Sci., Polym. Phys. Ed.*, **11**, 1385 (1973).
(5) K. Tai, M. Kobayashi, and H. Tadokoro, to be published.
(6) J. W. Leech, C. J. Peachey, and J. A. Reissland, *Phys. Lett.*, **10**, 69 (1964).
(7) J. W. Leech and J. A. Reissland, *J. Phys. C*, **3**, 975, 987 (1970).
(8) A. Warshel and S. Lifson, *J. Chem. Phys.*, **53**, 582 (1970).
(9) A. E. Smith, *J. Chem. Phys.*, **21**, 2229 (1953).
(10) M. Tasumi and T. Shimanouchi, *J. Chem. Phys.*, **43**, 1245 (1965).
(11) S. C. Nyburg and H. Lüth, *Acta Crystallogr., Sect. B*, **28**, 2992 (1972).
(12) J. H. Schachtschneider and R. G. Snyder, *Spectrochim. Acta*, **19**, 117 (1963).
(13) R. A. Scott and H. A. Scheraga, *J. Chem. Phys.*, **42**, 2209 (1965); **44**, 3054 (1966).
(14) I. Harada and T. Shimanouchi, *J. Chem. Phys.*, **44**, 2016 (1966); **46**, 2708 (1967).
(15) M. Kobayashi, K. Tashiro, and H. Tadokoro, *Macromolecules*, **8**, 158 (1975).
(16) M. Kobayashi, I. Okamoto, and H. Tadokoro, *Spectrochim. Acta*, in press.
(17) T. Kitagawa and T. Miyazawa, *Adv. Polym. Sci.*, **9**, 335 (1972).
(18) A. A. Maradudin, E. W. Montroll, and G. H. Weiss, "Theory of Lattice Dynamics in the Harmonic Approximation", Academic Press, New York, N.Y., 1963; *Solid State Phys., Suppl.*, **3**.
(19) L. P. Bouchaert, R. Smoluchowski, and E. Wigner, *Phys. Rev.*, **50**, 58 (1936).
(20) J. C. Slater, "Quantum Theory of Molecules and Solids", Vol. 2, McGraw-Hill, New York, N.Y., 1965.
(21) S. S. Chang, *J. Res. Natl. Bur. Stand., Sect. A*, **78**, 387 (1974).
(22) G. T. Davis, R. K. Eby, and J. P. Colson, *J. Chem. Phys.*, **41**, 4316 (1970).
(23) C. M. L. Atkinson and M. J. Richardson, *Trans. Faraday Soc.*, **65**, 1749 (1969).
(24) P. W. Teare and D. R. Holmes, *J. Polym. Sci.*, **24**, 496 (1957).
(25) C. M. L. Atkinson and M. J. Richardson, *Trans. Faraday Soc.*, **65**, 1764 (1969).
(26) G. Dean and D. H. Martin, *Chem. Phys. Lett.*, **1**, 415 (1967).
(27) R. T. Harley, W. Hayes, and J. F. Twisleton, *J. Phys. C*, **6**, L167 (1973).
(28) M. Kobayashi, T. Uesaka, and H. Yadokoro, to be published.
(29) L.-C. Brunel and D. A. Dows, *Spectrochim. Acta, Part A*, **30**, 929 (1974).
(30) H. Takeuchi, M. Tasumi, T. Shimanouchi, G. Vergoten, and G. Fleury, Symposium on Molecular Structures, Tokyo, 1974.
(31) J. E. Bertie and E. Whalley, *J. Chem. Phys.*, **41**, 575 (1964).


# Viscoelastic Properties of Homogeneous Triblock Copolymers of Styrene–α-Methylstyrene and Their Polyblends with Homopolymers


**David R. Hansen and Mitchel Shen***

*Department of Chemical Engineering, University of California, Berkeley, California 94720.*

*Received March 31, 1975*


ABSTRACT: Seven triblock copolymers of styrene–α-methylstyrene were prepared via anionic polymerization. Two types of block structures, ASA and SAS, were made. By the use of the Time Temperature Superposition Principle, stress relaxation isotherms of these block copolymers were readily shifted into smooth viscoelastic master curves. The shift factor data of all the block copolymers follow the classical WLF equation. Loss tangent data obtained by dynamic mechanical measurements show only one glass transition in each of these block copolymers, thus indicating the homogeneous nature of these materials. From the master curves, maximum relaxation times ($\tau_m$) were determined by the Procedure X method of Tobolsky and Murakami. These maximum relaxation times were found to vary as a function of copolymer composition and block structure. Comparison with $\tau_m$'s computed from molecular theory was satisfactory. Viscoelastic data of polyblends of the block copolymers with their respective homopolymers indicate that they are all homogeneous, except for the blend of an ASA triblock copolymer with poly(α-methylstyrene) which shows some signs of heterogeneity.


It is now well known that most block copolymers show microphase separation as a consequence of their positive free energy of mixing between the polymeric blocks. Because of this heterophase nature, many unique properties have been found to be dramatically different from those of the homogeneous homopolymers. For example, the viscoelastic behavior of heterophase block copolymers has been found to be thermorheologically complex.[1,2] However, a limited number of block copolymers are known to show no microphase separation, for example, the styrene–α-methylstyrene system.[3–6] It is therefore of interest to examine the properties of such homogeneous block copolymers in order to compare with those of the heterogenous ones.

An additional motivation to study these materials was provided by the recent interest in the molecular theoretical investigations of the viscoelastic properties of block copoly-